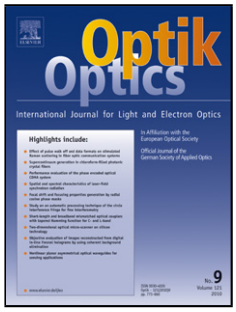

Title: Efficient Iris Localization and Recognition

Author: <ce:author id="aut0005" author-id="S0030402616314863-84404587f22b6d85f465bfb8663468c2"> Naglaa F. Soliman<ce:author id="aut0010" author-id="S0030402616314863-944891f83bd92ace5a66bb2143da4433"> Essam Mohamed<ce:author id="aut0015" author-id="S0030402616314863-ce9acbcc813071a87ea412783dc26990"> Fikri Magdi<ce:author id="aut0020" author-id="S0030402616314863-287edc1fbd1516315992cb35fd49b938"> Fathi E.Abd El-Samie<ce:author id="aut0025" author-id="S0030402616314863-056b6e9a707e24c496260268337b4df2"> AbdElnaby M

PII: S0030-4026(16)31486-3
DOI: http://dx.doi.org/doi:10.1016/j.ijleo.2016.11.150
Reference: IJLEO 58566

To appear in:

Received date: 11-1-2016
Accepted date: 28-11-2016

Please cite this article as: Naglaa F.Soliman, Essam Mohamed, Fikri Magdi, Fathi E.Abd El-Samie, AbdElnaby M, Efficient Iris Localization and Recognition, Optik - International Journal for Light and Electron Optics http://dx.doi.org/10.1016/j.ijleo.2016.11.150

Efficient Iris Localization and Recognition

Title page
Author Family Name Soliman

Given Name: Naglaa F.
Suffix Division: Department of Electronics and Electrical Communications, Faculty of Engineering, Zagazig University
Organization Zagazig University
Address Zagazig, Egypt
Email: nagla_soliman@yahoo.com

Author Family Name: Mohamed
Given Name: Essam
Suffix Division: Faculty of Engineering, Tanta University, Tanta, Egypt
Organization: Tanta University
Address: Tanta, Egypt
Email: m1_essam1@ieee.org

Author Family Name: Magdi
Given Name: Fikri.
Suffix Division: Department of Electrical Engineering and Electronics
Organization: Faculty of Engineering, Cairo University, Cairo, 32952, Egypt
Address: Cairo, 32952, Egypt
Email : magdi.fikri1@gmail.com

Author Family Name: El-Samie
Given Name: Fathi E. Abd
Suffix Division: Department of Electronics and Electrical Communications, Faculty of Electronic Engineering
Organization : Menoufia University
Address 32952, Menouf , Egypt
Email: fathi_syed@yahoo.com.

Author Family Name: M.
Given Name: AbdElnaby
Suffix Division: Smart Fields Production Technologist ,
Organization : Faculty of Engineering, Tanta University, Tanta, Egypt.
Address : Tanta, Egypt.
Email: mnaby1@yahoo.com.

ABSTRACT

Iris localization is an important step in iris recognition systems; all the subsequent steps, iris normalization, feature extraction and matching, depend on its accuracy. Traditional iris localization methods often involve an exhaustive search of a three-dimensional parameter space, which is a time consuming process. This paper presents a coarse-to-fine algorithm to address the computational cost problem, while achieving an acceptable accuracy. The iris gray image is transformed to a binary image using an adaptive threshold obtained from analyzing the image intensity histogram. Morphological processing is then used to extract an initial center point, which is considered as the initial center for both pupil and iris boundaries. Finally, a refinement step is made using an integro-differential operator to get the final iris and pupil centers and radii. This system proves to be robust against occlusions and intensity variations.

Keywords: *Biometrics, Iris localization, Image processing*.

I. INTRODUCTION

The recent advances of information technology and the increasing requirement for security have led to a rapid development of intelligent personal identification systems based on biometrics. Biometrics systems employ physiological or behavioral characteristics to accurately identify each subject. Biometric features include face, fingerprints, voice, iris, retina, gait, palm-prints, hand geometry, etc.

Among various approaches, iris-based personal recognition is referred to as the most promising one because of its high accuracy, good stability, and high recognition speed [1-3]. The details of the iris texture are believed to be different between persons and between the left and right eyes of the same person. The color of the iris can change as the amount of pigment in the iris increases during childhood. Nevertheless, for most of a human's lifespan, the

appearance of the iris is relatively constant[1].The first successful implementation of an iris recognition system was described by Daugman in 1993[4].

The iris is an annular part between the pupil (inner boundary) and the sclera (outer boundary) as shown in Fig. 1. Each boundary can be considered approximately as a circle, but they are not concentric. The iris localization algorithm aims to find the centers and the radii of the two boundaries to isolate the annular iris region from the original image. The localization accuracy has a great influence on the subsequent feature extraction and classification. As the localization result becomes more accurate, a high performance of feature extraction and recognition is achieved. Thus, iris localization plays a very important role in iris recognition and has stimulated a great deal of interests in recent years.

II. RELATED WORK

There are two classical iris localization methods. One was proposed by Daugman [4] , in which he used the integro-differential operator:

$$\max_{(r,x_0,y_0)} \left| G_\sigma(r) * \frac{\partial}{\partial r} \oint_{r,x_0,y_0} \frac{I(x,y)}{2\pi r} ds \right| \quad (1)$$

This operator searches the maximum angular integral of radial derivative over the image domain. It serves to find both the pupillary boundary and the outer (limbus) boundary of the iris. It is used initially to find the outer limbus boundary, where the angular arc of the contour is restricted in range to two opposing 90° centered on the horizontal meridian to avoid eyelids occlusion. Then, a second search begins within the limbus boundary to find the pupillary boundary, using a finer convolution scale σ. The other method was proposed by Wildes [3] and used later by Masek[5]. This method adopts the Hough transform to get iris boundaries after edge detection. Both methods need to search enormously in the three-dimensional parameter space, and hence they impose a great computational cost.

To improve the accuracy and speed of iris localization, different iris localization algorithms have been proposed in the recent years. In[6]and [7], active contours were used assuming a non-circular shape for the iris to get the actual shape and a better representation than a circle. However, if the iris edge details are weak, the contour evaluation may not stop at the desired iris boundary leading to an over-segmentation of the iris[7]. Other approaches use thresholding according to the image histogram, especially for pupil boundary; as it is relatively darker than the rest of the image such as the one proposed by SomnathDey and Debasis[8].

A coarse-to-fine strategy is proposed in this paper to reduce the computational cost. The Coarse stage aims to find an initial estimate to some of the two circles parameters.The fine stage refines these parameters usually with one of the two basic methods; circular Hough transform [9, 10] or integro-differential operator. More localization approaches are found in[11]and[12].

III. PROPOSED ALGORITHM

In this section, we discuss the proposed algorithm of iris localization. We have tried to combine the advantages of the other approaches to obtain a fast accurate algorithm, which is also robust to intensity variations and occlusions. The thresholding after intensity transformation approach was presented in[8]. It used a fixed threshold of 127. Thresholding results in fast processing, but the fixed threshold leads to problems in localization due to the varying illumination and occlusion conditions.

To solve this problem, the proposed algorithm uses thresholding with some morphological processing as an initial stage only. Also, histogram analysis is made for the CASIA-V3-Interval database images and a three-level thresholding system is introduced. The chosen threshold is used to transform the gray iris image into a binary image and separate the dark parts. Morphological processing is then applied and an approximated initial center value, which will be the pupil centroid, is obtained. This centroid will represent the base for our fine search for both pupil and iris boundaries.

Finally, the integro-differential operator will be used in an effective way to refine our final parameters. The image is resized to one quarter of its size and the search for the correct centers will be only in a neighborhood of 10×10 pixels around the initial center. In addition, two smaller sectors than those suggested by Daugman [4] are

used in the limbus boundary search with a certain radius range. This helps to obtain more accuracy and speed. The proposed algorithm is divided into two stages; coarse stage and fine stage.

A. Coarse Stage:

In this stage, a prior knowledge about the image acquisition system is assumed, which is the practical case. Histogram analysis led to the following three-level system threshold:

$$Threshold = \begin{cases} 115: \sum_{i=150}^{255} h_i > 0.75MN \\ 50: \sum_{i=0}^{100} h_i > 0.3MN \\ 85: otherwise \end{cases} \quad (2)$$

where h_i represents the histogram of the pixel intensity i, M is the number of image rows, and N is the number of image columns. The three-value thresholding makes the proposed algorithm suitable for bright, dark, and medium intensity conditions.The steps of the coarse stage can be summarized as follows:

1. Gray-scale closing with a disk structuring element to reduce the effect of eyelashes on the binary image result. Fig. 2(a) shows the result of closing of the sample image of Fig. 1 It is clear that the effect of eyelashes is reduced.
2. Choosing the suitable threshold according to Eq. (2).
3. Thresholding of the gray image and getting the binary output. This will show the darker parts of the image in white. These parts represent both the pupil and the remaining effects from eyelashes.
4. Filling the holes to reduce the effect of specular reflections on the pupil part from the Near Infra-Red (NIR) illuminators.
5. Labeling of connected areas and getting the maximum area that will represent the pupil region. The chosen area is considered as the pupil. Our initial center will be the centroid of this region.

Fig. 2(b) shows the resultant image after the thresholding and morphological operations. The pupil appears as the largest area and the centroid is marked as the initial center to the next stage. The success of this stage is achieved if the marked center falls in the pupil central area within a 10×10 neighborhood of the accurate centers.

B. Fine Stage

In this stage, Daugman's integro-differential operator in Eq. (1) is used twice for both the pupil boundary circle and the iris boundary circle, both circles are not concentric. This operator is accurate, because it searches over the image domain for the global maximum [11]. However, the problem is that this operator searches in a large-size three-dimensional parameter space. To solve this problem and reduce the computational cost, the following approach is used:

- The image is resized to one quarter of its size.
- Depending on the prior knowledge of the acquisition system, the radius search range is reduced.
- The coarse stage initial center helps us to search for the center in only a neighborhood of 10×10 pixels around this center. This neighborhood is sufficient as the iris and pupil centers are very close to each other and to the pupil centroid.
- In the iris boundary search, we search in two sectors not in the whole 360°. Both sectors extend from -30° to 30°, one for the left and the other for the right edge of the boundary. The origin point of both sectors is our centroid (initial center). This reduces the search cost and the noise created by eyelids and eyelashes.

After applying this stage, both circles and their corresponding centers are superimposed on the iris image as shown in Fig. 2(c). It is clear that the iris annular part is identified and can be easily isolated for the subsequent processes of the recognition system.

IV. Experimental Results

In our tests, the CASIA-V3 database[13] has been used as the pupil region is left unmasked instead of the uniform pupil circle in CASIA-V1, introducing the real challenge of specular reflections and nonuniform intensity. The proposed algorithm has been tested over 1817 iris images. These images are different snapshots for the left and right eyes of all the 249 subjects in the database taking a maximum of 5 images for the same eye. The algorithms have been implemented using MATLAB R2011b on a dual-core 1.7 GHz processor.

The results have been compared experimentally with Masek's open source code [5] , as the other algorithms details cannot be reached to be implemented faithfully. Since Masek's code applies Hough transform, it takes a long execution time, so we have applied it on only 100 images of 16 subjects taking a maximum of 5 images for the same eye.

The proposed algorithm takes *240 m*sec on average compared with *20 Sec* for Masek's code. To evaluate the accuracy of our localization, first a manual evaluation for the detected circles has been made depending on the appearance of the located iris. Our tests have been made on a large number of images with different intensity conditions. The localization results were robust to the heavy eyelashes occlusion and the varying intensity conditions. Fig. 3 shows some different results of these conditions.

Table 1 summarizes the accuracy rates achieved. The pupil boundary error is noticed in 15 images. The error in 14 images of them is attributed to a strong effect from specular reflections that causes the pupil area to be split after thresholding. The error in the remaining image causes is due to the connection between eyelashes and the pupil even after the closing processing. 7 images had iris boundary errors mainly due to the fine stage in the case of very weak iris edge details or the eyelashes effect. Fig. 4 shows samples of these errors. The total accuracy of Masek's code was 87%on average.

The second method of evaluating our algorithm is studying the effect of the localized iris result on the subsequent stages of feature extraction and matching. A simple recognition system from the existing techniques has been used in our evaluation. The localized iris has been normalized and then its features have been extracted as an iris template. The matching stage contains different comparisons for both genuine and imposter cases. After the recognition system has been built, the images with localization problems were tested to see the effect of these problems on the matching stage.

For the normalization, Daugman's rubber sheet model has been used [2]. The rubber sheet model remaps the iris image $I(x,y)$ from raw Cartesian coordinates (x,y) to the dimensionless nonconcentric polar coordinate system (r,θ) to overcome the pupil dilation and variation in size. Our system will produced a fixed normalized iris image of size 32 x 256.

In the feature extraction stage, Masek's method [5] with some modifications has been used. The features were obtained by convolving the normalized iris pattern with 1-D Log-Gabor wavelets. The 2-D normalized pattern was broken up into a number of 1-D signals, and then these 1-D signals were convolved with 1-D Gabor wavelets. The rows of the 2-D normalized pattern were taken as the 1-D signals, each row corresponds to a circular ring on the iris region. The angular direction was taken rather than the radial one, which corresponds to columns of the normalized pattern, since maximum independence occurs in the angular direction. The filter parameters suggested by Masek for CASIA database were used ($\lambda = 18$ and $bandwidth$ $parameter$ $\sigma = 0.5$).

Masek's code removes the noise created from eyelids and eyelashes by making a noise mask and finding the intersection between the mask and the template in the matching stage. In our tests, we simply removed the lower half of the normalized image and took only the features of the upper half, which correspond to the inner part close to the pupil boundary. So, the final normalized image was of size 16×256.

The output of filtering was then phase quantized to four levels using the Daugman's method [2]. This encoding system produced a bitwise template containing a number of bits of information equal to the angular resolution multiplied by the radial resolution, multiplied by 2 (i.e. $16 \times 256 \times 2 = 8192$ bits). Fig. 5 shows the normalized image and the resultant code for the localized iris of Fig. 2(c).

The matching technique depends on the Hamming Distance (HD) between the two iris templates *A*, *B* under comparison, which is calculated using the equation:

$$HD = \frac{1}{8192} \sum_{j=1}^{8192} A_j \, (xor) B_j \tag{3}$$

In our tests, 600 comparisons for genuine case (intra-class) and 600 comparisons for imposter case (inter-class) have been made. All the images used are correctly-segmented ones. The distribution of the HD is shown in bars in Fig. 6. The empirical distribution has a standard deviation of $\sigma = 0.0577, with\ a\ mean\ of\ \mu = 0.2948$ for the genuine case and $\sigma = 0.012, with\ \mu = 0.4747$ for the imposter case. These results were fitted to the Binomial distribution as proposed by Daugman [4] and shown as solid curves in Fig. 6.The number of equivalent Bernoulli trials (degrees of freedom) $N = \sigma^2/(p(1-p))p$ represents the average probability of not matching which is equivalent to the mean of each distribution. It has been found that $N = 1737$ for the imposter case and $N = 62$ for the genuine case.

The most important part of the analysis is to find the threshold that minimizes the matching errors. Table 2 shows the False Acceptance Rate (FAR) and False Reject Rate (FRR) for the empirical data and the corresponding Binomial distribution rate for each HD threshold. The best threshold for both errors is 0.44. However, the most costly error is the FAR and hence the threshold of 0.43 was used for our system.

The final part of our analysis is to try the 22 images with localization error in the recognition system and see how these errors affect the final decision. The 7 iris boundary problems were tested against all the available genuine images and 20 imposter comparisons for each image. There was only 1 false acceptance in the 140 imposter comparisons and 2 false rejections. We can see that the iris boundary problem has a low effect on the final result because of two reasons. Always the whole iris region lies within the detected boundary. Also, in our matching system we depend on the inner part close to the pupil.

For the 14 images with pupil boundary problem and the image with the two boundaries problem, there was almost complete failure in the genuine matching comparisons and the results are almost all false reject. This is due to the deviation in the pupil boundary, which is much more severe than the iris boundary problems, and also the dependence on the features near the pupil.

V. CONCLUSION

Iris localization is very important to the success of the next stages in the iris recognition system. The most important metrics of localization algorithm are accuracy and speed. In this paper, we focused on developing a fast iris localization algorithm, while preserving the accuracy compared to the other approaches. Thresholding is used as the first step instead of exhaustive search of a three-dimensional parameter space for a large number of image pixels. The proposed adaptive thresholding system has been used to overcome the varying illumination conditions. To guarantee an acceptable accuracy, the proposed algorithm fine stage used the known Daugman's integro-differential operator. It has been applied in two sectors, and in a specific radius range according to the database. We searched for the center parameters only in a neighborhood of 10×10 pixels around the initial center. The errors in the iris boundary have a low effect in the matching stage, whereas the pupil boundary problems result in false reject errors. The proposed algorithm leads to high processing speed, while keeping an acceptable accuracy compared to the other approaches.

REFERENCES

[1] K. W. Bowyer, K. Hollingsworth, and P. J. Flynn, "Image understanding for iris biometrics: A survey," *Computer Vision and Image Understanding,* vol. 110, pp. 281-307, May 2008.

[2] J. Daugman, "How iris recognition works," *IEEE Trans. Circuits Syst. Video Technol.,* vol. 14, pp. 21-30, Jan. 2004.

[3] R. P. Wildes, "Iris recognition: an emerging biometric technology," in *Proceedings of the IEEE*, 1997, pp. 1348-1363.

[4] J. G. Daugman, "High confidence visual recognition of persons by a test of statistical independence," *IEEE Trans. Pattern Anal. Mach. Intell.,* vol. 15, pp. 1148-1161, Nov. 1993.

[5] L. Masek, "Recognition of human iris patterns for biometric identification," M. Thesis, The University of Western Australia, 2003.

[6] J. Daugman, "New methods in iris recognition," *IEEE Trans. Syst., Man, Cybern., B,* vol. 37, pp. 1167-1175, Oct. 2007.

[7] S. Shah and A. Ross, "Iris segmentation using geodesic active contours," *IEEE Trans. Inf. Forensics Security,* vol. 4, pp. 824-836, Dec. 2009.

[8] S. Dey and D. Samanta, "A novel approach to iris localization for iris biometric processing," *International Journal of Biological and Medical Sciences,* vol. 3, 2008.

[9] L. Ma, T. Tan, Y. Wang, and D. Zhang, "Efficient iris recognition by characterizing key local variations," *IEEE Trans. Image Process.,* vol. 13, pp. 739-750, Jun. 2004.

[10] X. Feng, C. Fang, X. Ding, and Y. Wu, "Iris Localization with Dual Coarse-to-fine Strategy," in *18th International Conference on Pattern Recognition, ICPR 2006.* , 2006, pp. 553-556.

[11] R. Ng, Y. H. Tay, and K. M. Mok, "A review of iris recognition algorithms," in *International Symposium on Information Technology. ITSim 2008.* , 2008, pp. 1-7.

[12] Z. He, T. Tan, Z. Sun, and X. Qiu, "Toward accurate and fast iris segmentation for iris biometrics," *IEEE Trans. Pattern Anal. Mach. Intell.,* vol. 31, pp. 1670-1684, Sep. 2009.

[13] CASIA-IrisV3 Database [Online]. Available: http://www.cbsr.ia.ac.cn/english/IrisDatabase.asp

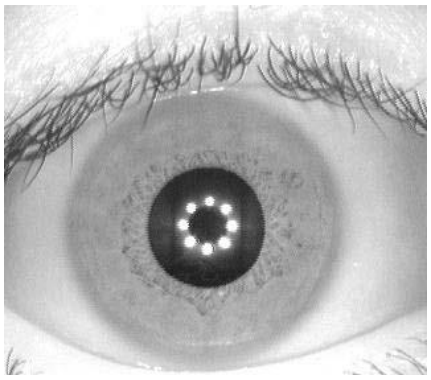

Fig. 1: Sample image from CASIA-IrisV3-Interval database.

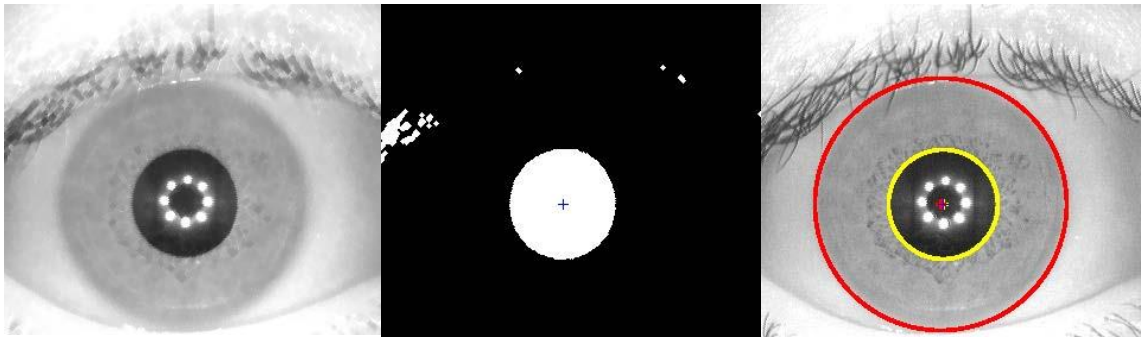

Fig. 2: Results of the proposed algorithm steps when applied to the image in Fig. 1. (a) Image after gray scale closing. (b) Image after thresholding and morphological processing with the centroid marked. (c) Final localized iris.

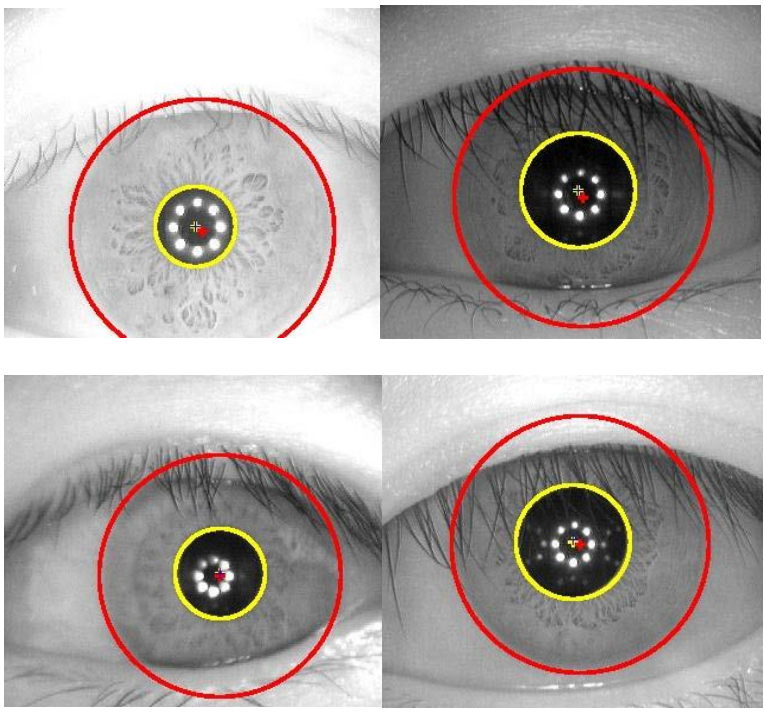

Fig.3: Different localization results showing the robustness of the proposed algorithm. (a) Bright image. (b) Dark image. (c) Heavy eyelashes occlusion. (d) Weak iris boundary details.

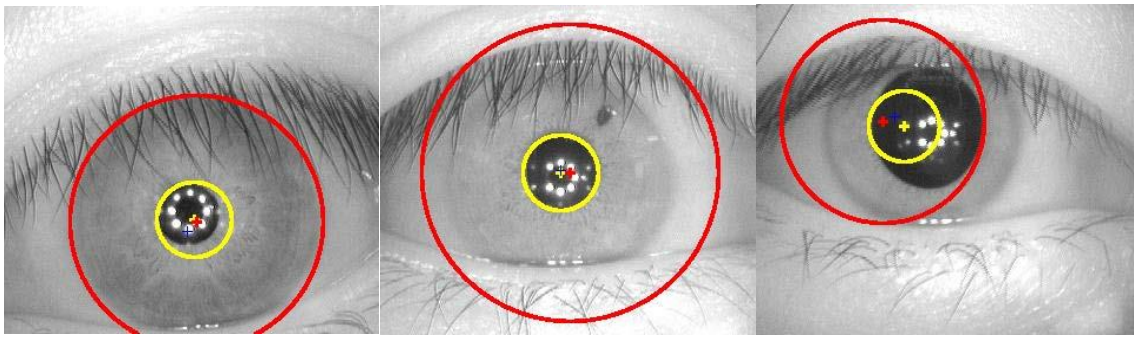

Fig.4: Examples for the three error types. (a) Pupil boundary error. (b) Iris boundary error. (c) Both boundaries error.

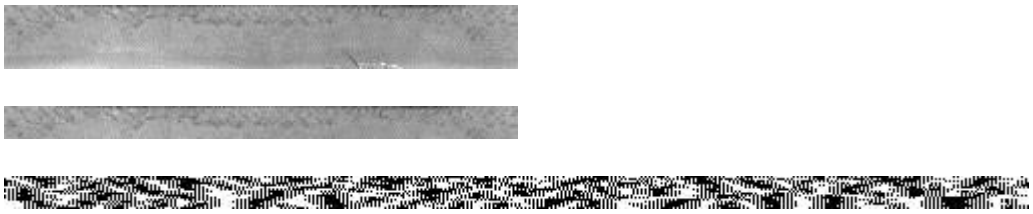

Fig. 5: Normalization and encoding steps. (a) Normalized image (32×256). (b) Upper half of the normalized image (16×256). (c) Resulting iris code.

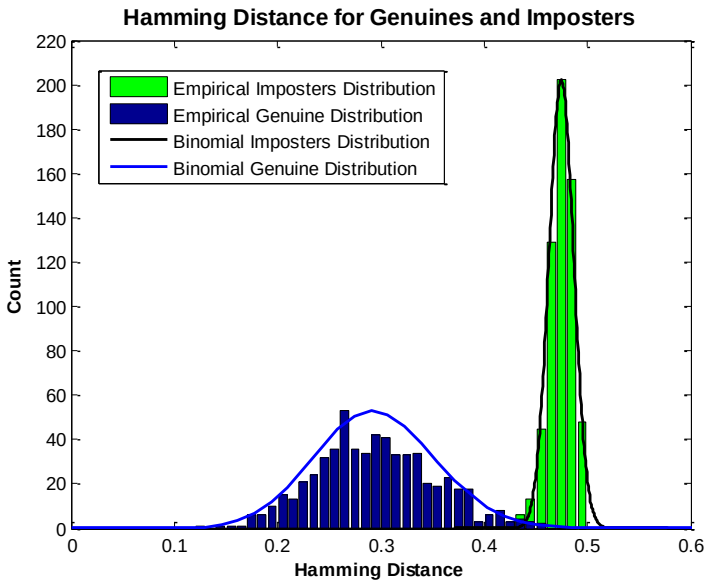

Fig. 6: Hamming distances for inter-class and intra-class comparisons.

Table 1: Accuracy of the proposed algorithm.

Pupil boundary accuracy	**Iris boundary accuracy**	**Total accuracy for both boundaries**
99.17%	99.93%	98.8%

Table 2: Performance of the matching system based on non-matching rates.

HD Threshold	**Empirical Results**		**Binomial Results**	
	FAR	**FRR**	**FAR**	**FRR**
0.43	0%	1.5%	0.007%	2.4%
0.44	1%	0.88%	0.16%	1.3%
0.45	3.17%	0.33%	1.9%	0.64%